



Inhibition of Ceramide Synthesis Ameliorates Glucocorticoid-, Saturated-Fat-, and Obesity-Induced Insulin Resistance

William L. Holland¹, Joseph T. Brozinick², Li-Ping Wang¹, Eric D. Hawkins², Katherine M. Sargent¹, Yanqi Liu¹, Krishna Narra¹, Kyle L. Hoehn¹, Trina A. Knotts¹, Angela Siesky², Don H. Nelson¹, Sotirios K. Karathanasis², Greg K. Fontenot³, Morris J. Birnbaum⁴ and Scott A. Summers¹  

¹Division of Endocrinology, Metabolism, and Diabetes, Department of Internal Medicine, University of Utah, Salt Lake City, UT 84132, USA

²Lilly Research Laboratories, Eli Lilly and Company, Indianapolis, IN 46285, USA

³Lexicon Genetics Incorporated, The Woodlands, TX 77381, USA

⁴Howard Hughes Medical Institute, University of Pennsylvania, Philadelphia, PA 19104, USA

Received 28 June 2006; revised 12 December 2006; accepted 10 January 2007.

Published: March 6, 2007. Available online 6 March 2007.

-

Referred to by: **The Path to Insulin Resistance: Paved with Ceramides?**, *Cell Metabolism*, Volume 5, Issue 3, 7 March 2007, Pages 161-163
Juleen R. Zierath
[SummaryPlus](#) | [Full Text + Links](#) | [PDF \(212 K\)](#)

-

Summary

Insulin resistance occurs in 20%–25% of the human population, and the condition is a chief component of type 2 diabetes mellitus and a risk factor for cardiovascular disease and certain forms of cancer. Herein, we demonstrate that the sphingolipid ceramide is a common molecular intermediate linking several different pathological metabolic stresses (i.e., glucocorticoids and saturated fats, but not unsaturated fats) to the induction of insulin resistance. Moreover, inhibition of ceramide synthesis markedly improves glucose tolerance and prevents the onset of frank diabetes in obese rodents. Collectively, these data have two important implications. First, they indicate that different fatty acids induce insulin resistance by distinct mechanisms discerned by their reliance on sphingolipid synthesis. Second, they identify enzymes required for ceramide synthesis as therapeutic targets for combating insulin resistance caused by nutrient excess or glucocorticoid therapy.

-**Author Keywords:** HUMDISEASE

-

Article Outline

[Introduction](#)

[Results](#)

[Ceramide Is an Obligate Intermediate Linking Glucocorticoids to the Induction of Insulin Resistance](#)

[Distinct Mechanisms for Saturated- and Unsaturated-Fat-Induced Insulin Resistance](#)

[Inhibiting Ceramide Synthesis Improves Glucose Tolerance and Prevents Diabetes in](#)

[Obese Rodents](#)

[Discussion](#)

[Experimental Procedures](#)

[Animal Surgery](#)

[Hyperinsulinemic-Euglycemic Clamps](#)

[DES1 Knockout Mice](#)

[Lipid Infusion](#)

[Isolated Muscles](#)

[Zucker Diabetic Fatty Rats](#)

[Analysis of Metabolites](#)

[Quantitative Real-Time PCR](#)

[Protein Analysis](#)

[Statistical Analysis](#)

[Acknowledgements](#)

[Supplemental Data](#)

[References](#)

-

Introduction

The peptide hormone insulin stimulates the uptake and storage of glucose and other nutrients in skeletal muscle and adipose tissue while simultaneously repressing glucose efflux from the liver. Insulin resistance occurs when a normal dose of the hormone is incapable of eliciting these anabolic responses, and the condition is a component of or risk factor for many metabolic diseases (e.g., diabetes, hypertension, atherosclerosis, cancer, etc.) ([Reaven, 2005](#)). Obesity predisposes individuals to the development of insulin resistance, and several mechanisms have been proposed to explain how increased adiposity antagonizes insulin stimulation of nutrient uptake and storage. First, increased adipose tissue mass may trigger the synthesis and/or secretion of glucocorticoids

([Hermanowski-Vosatka et al., 2005](#)) or inflammatory cytokines (e.g., tumor necrosis factor α [TNF α]) ([Hotamisligil, 2003](#)) that inhibit insulin action in peripheral tissues. Second, excess lipids may be delivered to nonadipose tissues that are not suited for fat storage (i.e., skeletal muscle and the liver), thus leading to the formation of specific metabolites that directly antagonize insulin action ([McGarry, 2002](#) and [Schmitz-Peiffer, 2000](#)).

The metabolic factors that induce insulin resistance almost invariably generate the sphingolipid ceramide ([Summers and Nelson, 2005](#)), which is a ubiquitous regulator of cellular stress ([Hannun and Obeid, 2002](#)). Moreover, studies in insulin-responsive cell types suggest that ceramide and/or its derivatives (e.g., ganglioside GM3 and sphingosine) antagonize insulin signaling, induce oxidative stress, and inhibit glucose uptake and storage, and thus may initiate many of the molecular defects that underlie insulin resistance ([Summers and Nelson, 2005](#)). An exciting theory that emerges from these observations is that the inhibition of ceramide synthesis could combat several underlying causes of insulin resistance and thus improve insulin sensitivity in tissues exposed to multiple different pathogenic factors associated with obesity. However, studies evaluating the relevance of ceramide to insulin resistance in vivo have been controversial. The debate stems from the fact that while ceramide accumulates in some insulin-resistant models ([Gorska et al., 2004](#), [Strackowski et al., 2004](#) and [Turinsky et al., 1990](#)), it fails to do so in lipid-infused animals ([Itani et al., 2002](#) and [Yu et al., 2002](#)). Moreover, the relative increase in ceramide in obese rodents and humans is typically rather small ([Adams et al., 2004](#) and [Turinsky et al., 1990](#)). Thus, some scientists have argued that it either is unimportant in lipid-induced insulin resistance or, alternatively, plays only a minor role in the regulation of glucose homeostasis following nutrient oversupply ([Itani et al., 2002](#) and [Yu et al., 2002](#)). To definitively address this issue, we investigated whether inhibiting ceramide synthesis improves glucose homeostasis in rodent models of insulin resistance, obesity, and diabetes.

Results

Ceramide Is an Obligate Intermediate Linking Glucocorticoids to the Induction of Insulin Resistance

Synthetic glucocorticoids (e.g., dexamethasone), one of the most frequently prescribed classes of therapeutics, impair glucose tolerance. This is particularly troublesome given the large number of insulin-resistant and/or diabetic individuals receiving these drugs. Though obese individuals do not have elevated glucocorticoid levels in the circulation, increased intracellular glucocorticoid tone—likely driven by increased activity of 11 β -hydroxysteroid dehydrogenase type 1, which converts inactive cortisone into active cortisol—causes insulin resistance in rodents and may contribute to the development of the disease in humans ([Kotelevtsev et al., 1997](#), [Kotelevtsev et al., 1999](#), [Masuzaki et al., 2001](#) and [Masuzaki et al., 2003](#)). As shown herein, dexamethasone stimulates ceramide biosynthesis by inducing expression of genes required for ceramide biosynthesis. The initial and rate-limiting reaction is the condensation of palmitoyl-CoA and serine, which is catalyzed by serine palmitoyltransferase (SPT), to produce 3-oxosphinganine ([Merrill,](#)

2002; see also [Figure S1](#) in the [Supplemental Data](#) available with this article online).

Three subsequent reactions follow, resulting in the production of sphinganine, dihydroceramide, and ultimately ceramide. Once generated, ceramide is the precursor of most active sphingolipids, including glucosylceramides, sphingosine, ceramide 1-phosphate, and sphingomyelin. Dexamethasone promoted ceramide accumulation in the portal circulation and the liver ([Figure 1A](#)). Moreover, it induced hepatic expression of serine palmitoyltransferase isoform 2 (SPT2) and (dihydro)ceramide synthases (i.e., longevity assurance gene homolog [LASS] 1 and 6) ([Figure 1B](#)). It also promoted expression of glucosylceramide synthase (GCS) and acid ceramidase (AC), suggesting that glucocorticoids may additionally increase formation of corresponding inhibitory sphingolipid metabolites such as ganglioside GM3 and sphingosine.

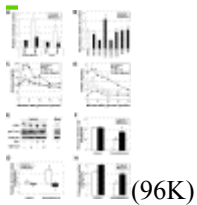


Figure 1. Ceramide Is a Requisite Intermediate Linking Dexamethasone to Insulin Resistance

(A) Sprague-Dawley rats were pretreated with myriocin (300 $\mu\text{g}/\text{kg}$, i.p.; solid bars) or saline (open bars) prior to administering dexamethasone (40 $\mu\text{g}/\text{kg}$, i.p.) or vehicle (5% ethanol in PBS). Mean ceramide levels from portal vein serum ($n = 9$) or nitrogen-pulverized liver ($n = 11$) are shown. To directly compare fold changes in ceramide levels within the liver and portal serum, values were normalized to those from untreated control samples (40.42 pmol/ μl for serum and 430 pmol/mg for liver). In this and all other figures, error bars represent $\pm\text{SEM}$.

(B) Protein (open bar) and mRNA (solid bars) were extracted and measured by western blotting and reverse-transcriptase PCR, respectively. Levels of transcripts encoding enzymes required for ceramide synthesis or metabolism are presented as the fold change in transcript or protein in dexamethasone-treated animals relative to vehicle controls. SPT2, LASS1, LASS6, GCS, and AC were significantly elevated in the dexamethasone-treated animals ($n = 5$).

(C and D) Rats were challenged with glucose (1 g/kg, i.p.) following treatment with dexamethasone (Dex, squares) or ethanol carrier (triangles) and/or myriocin (open shapes) or saline (solid shapes) as in (A). Tail-vein blood was sampled for glucose (C) and insulin (D) at the indicated times ($n = 6$).

(E) In animals treated with dexamethasone as above, insulin was injected into the portal vein as described previously ([Pagliassotti et al., 2002](#)). Livers were freeze clamped in situ, and PI3-kinase assays and western blots to detect phosphorylated (at serine 473) and total Akt/PKB were performed as described in [Experimental Procedures](#). Data are representative of six different independent experiments.

(F–H) Hyperinsulinemic-euglycemic clamps were performed on animals ($n = 9$ for myriocin-treated controls, $n = 6$ for other groups) treated as in (A) with myriocin (solid bars) or PBS (open bars). * $p < 0.05$ for dexamethasone-treated animals versus PBS-treated controls; † $p < 0.05$ for animals receiving myriocin + dexamethasone versus those receiving dexamethasone + vehicle. When comparing glucose and insulin levels during the glucose tolerance test, significance was determined using the area under the curve.

Concomitant with the increase in ceramide accumulation, dexamethasone mildly increased (13%) fasting blood glucose (Figure 1C) and induced a 2.8-fold increase in fasting insulin concentrations (Figure 1D). Furthermore, dexamethasone impaired glucose disposal (Figure 1C) and elevated insulin levels during the course of a glucose tolerance test (Figure 1D), suggestive of insulin resistance. Reducing ceramide levels with the SPT inhibitor myriocin (Figure 1A) significantly negated glucocorticoid-induced glucose intolerance (Figure 1C) and normalized circulating insulin concentrations following glucose challenge (Figure 1D).

Insulin tolerance tests suggested that dexamethasone impaired glucose homeostasis by decreasing insulin sensitivity, and this effect was fully negated by myriocin (Figure S2). To definitively evaluate effects on insulin sensitivity, as well as to distinguish whether our treatment protocols differentially affected glucose uptake in skeletal muscle or hepatic glucose output by the liver, we performed hyperinsulinemic-euglycemic clamps with D[U-¹⁴C]glucose and 2-deoxy-D[2,6-³H]glucose (2-DOG) tracers (Figure 1; Table 1). Dexamethasone decreased the glucose infusion rate required to maintain euglycemia (Figure 1F), prevented insulin-induced suppression of hepatic glucose output (Figure 1G), and inhibited 2-DOG uptake into skeletal muscle (Figure 1H). Pretreatment with myriocin partially blocked dexamethasone-induced insulin resistance in skeletal muscle and completely prevented the glucocorticoid's effects on hepatic glucose output. Neither dexamethasone nor myriocin affected rates of basal (non-insulin-stimulated) hepatic glucose output.

Table 1.

Plasma Components during Hyperinsulinemic-Euglycemic Clamp Studies

Dexamethasone Clamps						
Treatment		Before Clamp			During Clamp	
Dexamethasone	Myriocin	Glucose (mg/dl)	Insulin (ng/ml)	FFA (μ mol/l)	Glucose (mg/dl)	Insulin (ng/ml)
Control	Saline	121.2 \pm 5.4	1.12 \pm 0.32	240 \pm 27	129.2 \pm 2.8	5.8 \pm 0.9
	Myriocin	113.0 \pm 5.3	1.09 \pm 0.18	258 \pm 29	128.3 \pm 2.1	6.4 \pm 0.4
Dexamethasone	Saline	145.6 \pm 5.3*	4.50 \pm 1.76	211 \pm 38	132.2 \pm 3.4	6.8 \pm 1.1
	Myriocin	134.6 \pm 2.7*	2.34 \pm 0.44	176 \pm 34	127.4 \pm 2.9	5.7 \pm 1.4

Dexamethasone Clamps										
Treatment		Before Clamp			During Clamp					
Dexamethasone	Myriocin	Glucose (mg/dl)	Insulin (ng/ml)	FFA (μ mol/l)	Glucose (mg/dl)	Insulin (ng/ml)				
Lipid Infusion Clamps										
Treatment		Glucose (mg/dl)			Insulin (ng/ml)			FFA (mM)		
Lipid	Drug	Before Infusion	Before Clamp	During Clamp	Before Infusion	Before Clamp	During Clamp	Before Infusion	Before Clamp	During Clamp
Glycerol	PBS	123.9 \pm 6.9	113.9 \pm 2.4	114.3 \pm 3.6	0.59 \pm 0.16	1.33 \pm 0.32	5.66 \pm 1.07	0.55 \pm 0.06	0.52 \pm 0.04	0.23 \pm 0.05 ^a
	Myriocin	108.6 \pm 3.8	114.5 \pm 4.4	110.4 \pm 3.9	0.52 \pm 0.08	1.30 \pm 0.30	5.09 \pm 0.52	0.71 \pm 0.08	0.48 \pm 0.03	0.28 \pm 0.03 ^a
Lard oil	PBS	120.8 \pm 5.0	110.4 \pm 5.2	121.0 \pm 5.0	0.82 \pm 0.09	1.69 \pm 0.24	5.71 \pm 0.94	0.61 \pm 0.11	1.89 \pm 0.05 [*]	1.57 \pm 0.15 [*]
	Myriocin	98.2 \pm 6.6 [*]	105.5 \pm 5.0	122.5 \pm 0.9	0.62 \pm 0.09	2.00 \pm 0.53	4.73 \pm 0.88	0.76 \pm 0.20	2.12 \pm 0.32 [*]	1.87 \pm 0.29 [*]
Soy oil	PBS	116.4 \pm 10.7	116.2 \pm 4.8	121.6 \pm 4.9	0.97 \pm 0.03	1.94 \pm 0.40	6.00 \pm 1.24	0.52 \pm 0.07	2.24 \pm 0.40 [*]	1.59 \pm 0.36 [*]
	Myriocin	104.0 \pm 9.2	102.6 \pm 4.0	124.8 \pm 2.7 [*]	0.60 \pm 0.08 [†]	2.04 \pm 0.49	5.91 \pm 0.54	0.67 \pm 0.09	2.25 \pm 0.13 [*]	1.72 \pm 0.26 [*]

Dexamethasone clamps: Plasma parameters were assessed during hyperinsulinemic-euglycemic clamps of dexamethasone-treated Sprague-Dawley rats. Plasma was sampled from indwelling arterial lines before the infusion of insulin or during a 60 min euglycemic steady state. Glucose was analyzed using a Beckman Glucose Analyzer II approximately every 7 minutes throughout the steady-state period. Insulin was analyzed by ELISA from two steady-state samples. Free fatty acid (FFA) was measured using the colorimetric half-micro test from Roche. (n = 9 for myriocin-treated animals; n = 6 for other groups.) * p < 0.05 versus saline-injected controls. Lipid infusion clamps: Plasma parameters were assessed during hyperinsulinemic-euglycemic clamps of lipid-infused Sprague-Dawley rats. Plasma was sampled from indwelling arterial lines before the infusion of lipid, before coinfusion of insulin, or during a 30 min euglycemic steady state. Glucose was analyzed using a Beckman Glucose Analyzer II approximately every 5 minutes throughout the steady-state period. Insulin was analyzed by ELISA from terminal plasma samples. FFA was measured using the colorimetric half-micro test from Roche. * p < 0.05 versus PBS-treated, glycerol-infused controls (n = 6); † p < 0.05 for animals receiving myriocin versus vehicle-treated animals undergoing an otherwise identical treatment regimen (n = 6).

^a FFA levels obtained during the clamp were significantly different from those found just prior to initiating the clamp.

We and others have demonstrated previously that ceramide antagonizes insulin stimulation of glucose uptake and glycogen synthesis by inhibiting phosphorylation and activation of Akt/protein kinase B (PKB) ([Hajduch et al., 2001](#), [Powell et al., 2003](#), [Stratford et al., 2004](#), [Summers et al., 1998](#) and [Teruel et al., 2001](#)), a central mediator of insulin's anabolic effects. In these prior studies, ceramide failed to inhibit phosphatidylinositol 3-kinase (PI3-kinase), an obligate intermediate in the signaling pathway linking insulin to the stimulation of Akt/PKB. We thus tested whether dexamethasone and myriocin altered the phosphorylation of Akt/PKB on serine 473, an important regulatory residue in the enzyme's C terminus. Treating rats with dexamethasone markedly impaired insulin stimulation of Akt/PKB in the liver without affecting PI3-kinase ([Figure 1E](#)). Myriocin completely negated this dexamethasone effect. Myriocin similarly negated dexamethasone inhibition of Akt/PKB in soleus muscle ([Figure S2B](#)). Collectively, these data support the hypothesis that ceramide inactivation of Akt/PKB is a contributing mechanism by which the sphingolipid impairs insulin action.

To substantiate the data obtained with myriocin, we tested whether the genetic ablation of one or both alleles of dihydroceramide desaturase 1 (*Des1*) (GenBank accession number [NM_007853](#)), which encodes the enzyme that converts metabolically inactive dihydroceramide into active ceramide ([Figures S3A and S3B](#)), markedly altered tissue sphingolipid levels and glucose homeostasis. Homozygous null (*Des1*^{-/-}) pups contained no detectable DES1 protein and much less ceramide, but dramatically more dihydroceramide ([Figure 2B](#)), than wild-type (*Des1*^{+/+}) or heterozygous (*Des1*^{+/-}) littermates. Moreover, heart, liver, pancreas, white adipose tissue (WAT), and soleus muscle obtained from 7-week-old *Des1*^{-/-} animals contained no detectable ceramide levels (n = 3; p < 0.01), while those dissected from *Des1*^{+/-} mice had a markedly reduced ratio of active ceramide to inactive dihydroceramide ([Figure 2C](#)).

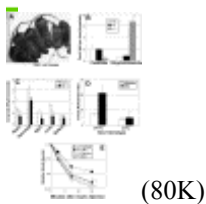


Figure 2. Mice Lacking Dihydroceramide Desaturase 1 (DES1) Are Resistant to Dexamethasone-Induced Insulin Resistance

(A) Mice lacking DES1 were generated as described in [Experimental Procedures](#). Mice lacking one allele (*Des1*^{+/-}) were indistinguishable from wild-type (*Des1*^{+/+}) animals, while those lacking both alleles (*Des1*^{-/-}) had a markedly different phenotype described in the text.

(B) Whole-body ceramide and dihydroceramide were quantified by mass spectrometry from 1-day-old *DesI*^{+/+} (open bars), *DesI*^{+/-} (solid bars), or *DesI*^{-/-} (hatched bars) mice (n = 5).

(C) Ceramide and dihydroceramide were quantified by mass spectrometry from individual tissues isolated from 7-week-old *DesI*^{+/+} (open bars) or *DesI*^{+/-} (solid bars) mice (n = 5).

(D) Fasting insulin resistance indices were calculated from mice treated for 1 week with dexamethasone (Dex, 2 mg/kg/day, i.p.; solid bars) or vehicle (open bars) (n = 4). Differences were assessed by comparing total area under the curve.

(E) Insulin tolerance tests were initiated by injection of insulin (0.75 mU/kg, i.p.) into *DesI*^{+/+} (squares) or *DesI*^{+/-} (triangles) mice treated with dexamethasone (2 mg/kg/day, 10 days; dashed lines, filled shapes) or PBS (solid lines, open shapes). Data are presented as the mean glucose level normalized to the fasting glucose concentration (n = 5). *p < 0.05 versus wild-type littermates; †p < 0.05 for heterozygous mice receiving dexamethasone versus wild-type animals undergoing the same treatment regimen.

The homozygous null *DesI*^{-/-} mice revealed an incompletely penetrant lethality ([Figure S3C](#)). Surviving animals were small in size ([Figure S4B](#)) with a complex phenotype, including scaly skin and sparse hair ([Figure 2A](#)), tremors, and numerous blood chemistry and hematological abnormalities. The homozygous null mice also exhibited signs of growth retardation when compared with their wild-type littermates, including notably decreased mean body weight and length, total tissue mass, lean body mass, and bone mineral content and density measurements. In addition, these mutants exhibited abnormal liver function test results, including increased mean serum alkaline phosphatase, alanine aminotransferase, and total bilirubin levels. The animals ultimately failed to thrive, dying within 8 to 10 weeks of birth. The heterozygous *DesI*^{+/-} animals were born at Mendelian ratios and demonstrated no obvious health abnormalities. Although ceramide has been implicated in immune cell function, neither the *DesI*^{-/-} nor *DesI*^{+/-} animals displayed alterations in circulating white blood cells, lymphocytes, or neutrophils (data not shown).

Because of the sickly nature of the homozygous null *DesI*^{-/-} mice, we restricted our analysis of glucose metabolism to the heterozygous *DesI*^{+/-} animals. When compared to wild-type *DesI*^{+/+} littermates, the *DesI*^{+/-} animals had normal glucose tolerance (data not shown) but demonstrated enhanced insulin sensitivity ([Figures 2D](#) and [2E](#)). Moreover, they were refractory to dexamethasone-induced insulin resistance ([Figures 2D](#) and [2E](#)). These studies strongly support the conclusion that ceramide synthesis is requisite for glucocorticoid-induced insulin resistance.

Distinct Mechanisms for Saturated- and Unsaturated-Fat-Induced Insulin Resistance

An additional mechanism by which insulin resistance likely develops in the obese is through the accumulation of fats in tissues not suited for lipid storage ([McGarry, 2002](#)). To mimic this condition in rats, we delivered a 20% lard-oil/heparin infusate into the bloodstream of Sprague-Dawley rats via jugular catheters. As compared to a 2.5%

glycerol infusate, lard-oil infusion increased serum free fatty acid (FFA) concentrations ([Table 1](#)) and promoted ceramide accrual in skeletal muscle ([Figure 3E](#)) and liver (249 ± 29 pmol/mg for glycerol versus 401 ± 72 pmol/mg for lard oil; $n = 9$; $p < 0.05$). It also stimulated formation of diacylglycerol (DAG), a glycerolipid previously implicated in lipid-induced insulin resistance ([Figure 3F](#)) ([Yu et al., 2002](#)). To assess muscle insulin sensitivity during the infusion, hyperinsulinemic-euglycemic clamps were performed on conscious, unrestrained rats during the terminal 90 min of the protocol. Lard-oil infusion decreased the glucose infusion rate required to maintain euglycemia to 19% of glycerol-treated control subjects ([Figure 3A](#)), increased hepatic glucose output ([Figure 3B](#)), and inhibited whole-body 2-DOG uptake ([Figure 3C](#)). Moreover, it inhibited insulin stimulation of Akt/PKB ([Figure 3D](#)). However, the inclusion of myriocin, which blocked ceramide synthesis in soleus muscle ([Figure 3E](#)) and liver (118 ± 38 pmol/mg for lard oil; $n = 6$; $p < 0.05$ versus vehicle control), negated these lard-oil effects ([Figures 3A–3C](#)). Differences in the glucose infusion rate could not be accounted for by the slight differences in the glucose concentration that were achieved during the clamp or differences in steady-state insulin or fatty-acid concentrations ([Table 1](#)). Neither lard oil nor myriocin affected rates of basal (non-insulin-stimulated) hepatic glucose output. Myriocin did not reduce levels of DAG ([Figure 3F](#)), indicating that ceramide, and not DAG, is the primary regulator of insulin resistance induced by this lard-oil cocktail. Moreover, myriocin failed to prevent lipid induction of TNF α and interleukin-6, two inflammatory cytokines previously implicated in lipid induction of insulin resistance. Thus, myriocin works either independently or downstream of these inflammatory modulators.

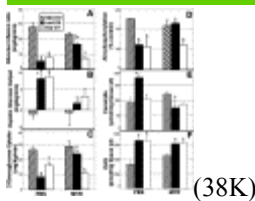


Figure 3. Ceramide Is Requisite for Lard-Oil- but Not Soy-Oil-Induced Insulin Resistance

Glycerol (hatched bars), lard oil (solid bars), or soy oil (open bars) was intravenously infused in rats for 6 hr in the presence or absence of myriocin (MYR).

(A–C) Hyperinsulinemic-euglycemic clamps were initiated after 4.5 hr of infusion, and the mean glucose infusion rate, hepatic glucose output, and 2-deoxyglucose (2-DOG) uptake were quantified as described in [Experimental Procedures](#) ($n = 6$).

(D) Lipid-infused animals were stimulated with insulin (10 mU/kg/min) under euglycemic conditions. Following 30 min of insulin coinfusion, rats were anesthetized with pentobarbital, and soleus muscles were freeze clamped in situ. Phosphorylation of Akt/PKB was assessed by western blot using phosphospecific antibodies recognizing the activating serine 473 site. Values were normalized to total Akt/PKB protein present in the lysates, which was unchanged by any of the treatment protocols. Data are presented as normalized to glycerol controls ($n = 6$).

(E and F) Ceramide (E) and diacylglycerol (DAG, F) levels in soleus muscles undergoing the treatment protocol described in (D) were quantified as described previously ([Chavez et al., 2003](#)) ($n = 6$). * $p < 0.05$

versus control animals infused with glycerol + vehicle; †p < 0.05 for myriocin-infused animals versus vehicle-treated animals undergoing an otherwise identical treatment regimen.

Many studies investigating acute effects of lipids on insulin action have involved the infusion of Intralipid or Liposyn II ([Boden and Shulman, 2002](#), [Kim et al., 2004](#), [Kim et al., 2001](#), [Kim et al., 2002](#) and [Yu et al., 2002](#)), which are soy-based lipid cocktails enriched in the unsaturated fat linoleate but low in the saturated fatty acids required for synthesis of the sphingosine backbone of ceramide ([Chavez and Summers, 2003](#)). As shown previously, soy-oil (i.e., Intralipid) infusion decreased the glucose infusion rate required to maintain euglycemia and inhibited whole-body 2-DOG uptake ([Figures 3A and 3C](#)) without inducing ceramide accumulation ([Yu et al., 2002](#)) ([Figure 3F](#)). Like lard oil, however, it markedly elevated circulating FFAs ([Table 1](#)), inhibited insulin stimulation of Akt/PKB ([Figure 3D](#)), and increased muscle DAG levels ([Figure 3F](#)). Myriocin did not prevent Intralipid-induced DAG accumulation ([Figure 3E](#)) or insulin resistance ([Figures 3A, 3C, and 3D](#)), confirming that soy-based cocktails induce insulin resistance in muscle by a ceramide-independent mechanism. Although the soy-oil infusion failed to induce ceramide, myriocin treatment alone decreased hepatic ceramide levels to 27% of saline-treated controls. Interestingly, this reduction in liver ceramide partially restored insulin suppression of hepatic glucose output.

The differential sensitivity of the lard- and soy-oil emulsions to inhibitors of ceramide synthesis suggests that different fatty acids may induce insulin resistance in muscle by distinct mechanisms. To test this hypothesis, we evaluated whether insulin resistance induced by saturated (palmitate) or unsaturated (linoleate) FFAs, which differ in abundance in the cocktails and in their capacity to generate ceramide, demonstrated a differential sensitivity to inhibitors of ceramide synthesis. Following completion of a 6 hr incubation, both palmitate and linoleate inhibited insulin-stimulated 2-DOG uptake ([Figure 4C](#)) and induced DAG accrual ([Figure 4B](#)) in isolated muscle strips. However, palmitate, but not linoleate, promoted ceramide accumulation ([Figure 4A](#)). To ascertain whether ceramide selectively mediated the antagonistic effects of palmitate, identical groups of muscles were treated with myriocin (10 μ M) or cycloserine (1 mM), a structurally unrelated inhibitor of serine palmitoyltransferase. Both compounds prevented palmitate-induced ceramide accumulation without affecting DAG ([Figures 4A and 4B](#)), and the inclusion of either drug completely negated the antagonistic effects of palmitate on insulin-stimulated 2-DOG uptake ([Figure 4C](#)). By contrast, these compounds did not alter linoleate effects on DAG accumulation ([Figure 4B](#)) or 2-DOG uptake ([Figure 4C](#)). Results obtained using muscles isolated from the aforementioned knockout mice further supported the hypothesis, as the *DesI*^{+/-} animals were resistant to palmitate antagonism of 2-DOG uptake but were fully inhibited by linoleate ([Figure 4D](#)).

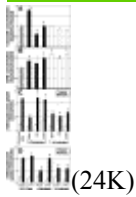


Figure 4. Ceramide Is Essential for Palmitate- but Not Linoleate-Induced Insulin Resistance

(A–C) Soleus muscles were isolated, bisected, and placed in oxygenated Krebs-Henseleit buffer containing 2.5% FFA free bovine serum albumin (BSA, hatched bars), 1 mM palmitate (solid bars), or 1 mM linoleate (open bars). Indicated muscle strips were maintained in the presence of cycloserine (CS, 1 mM) or myriocin (MYR, 10 μ M) throughout the experiments. Ceramide (A) and DAG (B) were enzymatically quantified, and data were normalized to the BSA-treated muscle strip from the same rat. 2-DOG uptake (C) was measured as previously described ([Brozinick and Birnbaum, 1998](#)) in the absence (open bars) or presence of insulin (300 μ U/ml; solid bars) during the final 20 min of the 6 hr incubation.

(D) Intact soleus muscles were dissected from 15- to 20-week-old *DesI*^{+/-} and *DesI*^{+/+} mice and incubated for 6 hr in lipid (1 mM) as indicated. During the final hour of the incubation, muscles were treated with or without insulin (300 μ U/ml). 2-DOG uptake was assessed as in (C). **p* < 0.05 versus BSA-treated controls (*n* = 6); †*p* < 0.05 for muscles receiving myriocin or cycloserine versus vehicle-treated muscles undergoing an otherwise identical treatment regimen (*n* = 6); ‡*p* < 0.05 for muscles from *DesI*^{+/-} animals versus muscles from *DesI*^{+/+} animals undergoing an otherwise identical treatment regimen (*n* = 6). Note: for 2-DOG uptake experiments, statistical comparisons were made only for insulin-treated samples. 2-DOG uptake rates in muscles not receiving insulin are included for reference purposes.

Inhibiting Ceramide Synthesis Improves Glucose Tolerance and Prevents Diabetes in Obese Rodents

We next asked whether modulating ceramide levels could be an effective therapeutic strategy for combating insulin resistance and glucose intolerance in rodent models of obesity. Zucker diabetic fatty (ZDF) rats, which become diabetic at 10–11 weeks of age, and lean controls were given myriocin for up to 6 weeks. As in prior studies ([Hojjati et al., 2005](#) and [Park et al., 2004](#)), the compound was well tolerated, as it had no effect on body mass ([Figure S5A](#)) or epididymal fat mass ([Figure S5B](#)) and no apparent side effects. As predicted, animals treated with vehicle demonstrated a progressive increase in plasma glucose ([Figure 5A](#)) and triglycerides ([Figure 5B](#)). Moreover, these animals failed to maintain the compensatory hyperinsulinemia seen in early stages of glucose intolerance, and the disease progressed as circulating insulin levels fell ([Figure 5C](#)). Treatment with myriocin, starting at week 8, prevented the onset of diabetes, as evidenced by the reduced glucose and triglyceride levels in the drug-treated animals ([Figures 5A and 5B](#)). The improvement in blood glucose levels persisted until the animals were at least 16 weeks in age (data not shown). Ceramides were elevated in soleus muscle ([Figure 5D](#)), liver ([Figure 5E](#)), and serum ([Figure 5F](#)) of the ZDF rats, and myriocin reduced levels of the sphingolipid in all of these tissues. Myriocin improved glucose tolerance and lowered insulin levels in the ZDF rats ([Figures 6A and 6B](#)) and improved insulin sensitivity as measured by insulin tolerance tests ([Figure 6C](#)). Zucker

fa/fa rats (Figure S6) also showed improvement in glucose tolerance when treated with myriocin. Similarly, myriocin reduced insulin levels after glucose challenge in diet-induced obese mice with normal glucose tolerance (Figure S7), which suggests improved insulin sensitivity. Collectively, these data identify ceramide synthesis inhibition as a therapeutic strategy for combating insulin resistance associated with excessive nutrient intake.

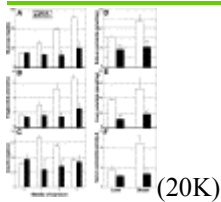


Figure 5. Myriocin Improves Glucose Homeostasis and Prevents Diabetes in ZDF Rats

(A–C) Myriocin administered via either oral gavage (0.5 mg/kg/day) or intraperitoneal injection (0.3 mg/kg every other day, i.p.) markedly improved glucose homeostasis in male ZDF rats. Seven-week-old animals were assigned to vehicle (1% w/v carboxymethylcellulose, 0.25% Tween 80; open bars) or myriocin (oral gavage; solid bars) groups based on starting plasma glucose levels and body weight. Blood samples were obtained 1 hr postdose at the indicated days from the tail vein of conscious animals by gentle massage following tail snip. Plasma was used for measurements of glucose (A), triglyceride (B), and insulin levels (C) (n = 5).

(D–F) Ceramide was measured enzymatically from soleus muscle (D), liver (E), or serum (F) of lean or obese ZDF rats following treatment with myriocin (0.3 mg/kg every other day, i.p.; solid bars) or saline (open bars) from age 7 weeks through 15 weeks. †p < 0.05 for myriocin-treated animals versus vehicle-treated animals undergoing an otherwise identical treatment regimen; *p < 0.05 versus lean controls (n = 4).

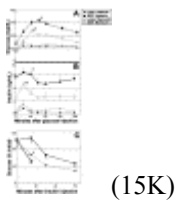


Figure 6. Myriocin Improves Glucose Tolerance in ZDF Rats

Seven-week-old male ZDF (squares) and lean (triangles) rats were dosed with myriocin (300 µg/kg in saline; open symbols) or saline (closed symbols) every other day.

(A and B) Following 10 days of myriocin treatment, overnight-fasted rats were challenged with an oral dose of glucose (2.5 g/kg, oral gavage). Glucose was measured by glucometer on whole-blood samples obtained from a tail nick. Serum was collected at the indicated time points, and insulin was measured by ELISA (n = 4).

(C) Insulin tolerance tests were initiated by insulin injection (2 U/kg, i.p.) following an overnight fast in 11-week-old nondiabetic ZDF rats. Glucose injections were given after 15 min to lean controls to rescue from hypoglycemia. Data are presented as the mean glucose normalized to initial glucose. (n = 4). *p < 0.05

versus lean animals; † $p < 0.05$ for myriocin-treated samples versus vehicle-treated animals undergoing the same treatment regimen.

Discussion

A collision of genetic and environmental factors has produced an epidemic growth of obesity and insulin-resistance rates during the last decade. As a result, prognosticators estimate that life expectancy, which has risen steadily over the last two centuries, may soon start to decline ([Olshansky et al., 2005](#)). In humans, the development of insulin resistance is likely caused by a diverse range of factors (nutrients, inflammatory cytokines, and glucocorticoids) that are influenced by obesity and a sedentary lifestyle. Ceramide is a candidate molecular intermediate linking many of these metabolic stresses to the induction of insulin resistance ([Summers and Nelson, 2005](#)), and the sphingolipid accumulates in insulin-resistant humans ([Adams et al., 2004](#)). Herein, we demonstrate that ceramide synthesis is an important component of insulin resistance triggered by at least two different pathogenic insults (i.e., glucocorticoids and saturated fatty acids). Moreover, inhibition of ceramide biosynthesis markedly improved glucose homeostasis in rodent models of obesity and diabetes. Thus, excess accumulation of ceramide and/or its metabolites likely underlies the antagonism of insulin signaling that leads to insulin resistance.

The studies presented have additional implications toward our understanding of the pathology of insulin resistance caused by lipid oversupply. Findings obtained using lipid-infusion protocols have suggested that DAG, and not ceramide, is the primary mediator of lipid-induced insulin resistance ([Itani et al., 2002](#) and [Yu et al., 2002](#)). We can explain differences between our study and previous ones by demonstrating that ceramide synthesis is dispensable for insulin resistance caused by unsaturated fats (e.g., linoleate), which do not drive ceramide synthesis. By contrast, ceramide is a requisite intermediate linking saturated fatty acids (i.e., palmitate) to the antagonism of insulin action. Thus, these findings provide definitive evidence that different fatty acids antagonize insulin-stimulated glucose uptake by distinct mechanisms discerned by their intracellular routes of metabolism and that prior studies relying on lipid cocktails comprised predominantly of unsaturated fatty acids may have underappreciated the roles of ceramides in insulin resistance. Since both dietary and epidemiological studies strongly implicate saturated fats, which are more poorly oxidized than unsaturated fats ([Gaster et al., 2005](#)), in the induction of human insulin resistance ([Rivellese and Lilli, 2003](#)), modulators of ceramide may prove useful for combating insulin resistance caused by oversupply of saturated fats. Supporting this conclusion are studies in rodents and humans indicating that ceramide inversely correlates with insulin sensitivity ([Adams et al., 2004](#) and [Straczkowski et al., 2004](#)) and that exercise decreases ceramide in concert with its beneficial effects on insulin action ([Dobrzyn et al., 2004](#) and [Helge et al., 2004](#)).

Our findings identify both the liver and skeletal muscle as targets of ceramide-induced insulin resistance. Surprisingly, however, we observed that dexamethasone induced a

striking increase in ceramide within the portal vein. This curious observation suggests that circulating ceramide, rather than ceramide derived from endogenous lipid stores, may be an important modulator of insulin sensitivity in the liver. One hypothesis is that ceramide generated in and secreted from visceral WAT modulates insulin sensitivity and glucose output from the liver as a mechanism for communicating nutrient status or energy need. For example, during periods of acute stress, glucocorticoids might trigger the synthesis and secretion of ceramide from WAT, which would decrease hepatic insulin sensitivity and increase the amount of glucose available for glycolysis. In obese states, increased nutrient load coupled with WAT inflammation would greatly augment ceramide synthesis in WAT, which could contribute to the sustained insulin resistance that underlies the metabolic syndrome. In this scenario, ceramide synthesis in other tissues (e.g., skeletal muscle, vascular endothelial cells, pancreatic β cells, etc.) may underlie pathogenic responses to hyperlipidemia but not be a factor in early stages of obesity-induced glucose intolerance. Elucidation of this mechanism will require novel experimental strategies to ablate ceramide synthesis in a tissue-specific manner.

Studies in cultured cells suggest that the primary mechanism by which ceramide antagonizes insulin action is through the inhibition of Akt/PKB ([Chavez et al., 2003](#), [Chavez et al., 2005](#), [Hajduch et al., 2001](#), [Powell et al., 2003](#), [Powell et al., 2004](#), [Summers et al., 1998](#), [Teruel et al., 2001](#) and [Wang et al., 1998](#)). Data presented herein are consistent with this mechanism, as ceramide depletion restored signaling to Akt/PKB in both dexamethasone- and lard-infused animals. Ceramide appears to block Akt/PKB activation through two independent pathways. First, ceramide catalyzes the dephosphorylation of Akt/PKB by activating protein phosphatase 2A ([Chavez et al., 2003](#), [Stratford et al., 2004](#) and [Teruel et al., 2001](#)). Second, ceramide blocks Akt/PKB translocation to the plasma membrane ([Stratford et al., 2001](#)). Studies by the Hundal laboratory reveal that protein kinase C ζ , which is also activated by ceramide, may intermediate this ceramide effect by phosphorylating Akt/PKB on an inhibitory residue within the enzyme's pleckstrin homology domain, thus preventing its interactions with 3'-phosphoinositides ([Powell et al., 2003](#) and [Powell et al., 2004](#)).

The ceramide-independent mechanism by which unsaturated fatty acids (e.g., linoleate) antagonize insulin signaling remains less clear. DAG has been proposed to mediate the effects of this lipid cocktail ([Yu et al., 2002](#)), by activating PKC θ , which phosphorylates and inactivates IRS-1 ([Kim et al., 2004](#)). However, we have demonstrated in [Chavez et al. \(2003\)](#) and herein that DAG produced by incubating cells or isolated muscles ([Figure 3](#)) in palmitate is insufficient to inhibit insulin signaling. One possible explanation for this discrepancy is that DAG comprised of the linoleate acyl chain (18:2) is a more potent activator of this pathway than DAG derived from saturated fats. Indeed, [Wakelam \(1998\)](#) described numerous experimental findings supporting the hypothesis that polyunsaturated forms of DAG, and not saturated derivatives, serve as intracellular signals.

In summary, using an array of pharmacological and genetic tools to modulate ceramide levels in rodents, we have demonstrated the following herein: first, ceramide is a common molecular intermediate linking both glucocorticoids and saturated fatty acids to

the induction of insulin resistance; second, different fatty-acid classes antagonize insulin-stimulated glucose uptake by distinct mechanisms distinguished by their dependence upon ceramide synthesis; and third, manipulating ceramide levels in obese rodents ameliorates insulin resistance and blocks the onset of diabetes. Collectively, these studies identify enzymes involved in ceramide biosynthesis as therapeutic targets for combating insulin resistance caused by glucocorticoid therapy or obesity.

Experimental Procedures

Animal Surgery

For lipid infusion and hyperinsulinemic-euglycemic clamp protocols, animals were anesthetized with ketamine (65 mg/kg) and xylazine (10 mg/kg), and polyethylene catheters were aseptically placed in the left carotid artery (advanced to the aortic arch) or the right jugular vein. Catheters were filled with 3% heparinized saline to maintain patency and exteriorized in the intrascapular region. Buprenorphine (0.03 mg/kg, s.c.) was postsurgically administered for pain control, and animals were allowed to recover (5–7 days) to preoperative weight prior to experiments.

Hyperinsulinemic-Euglycemic Clamps

Clamps were performed in conscious unrestrained animals using swivels and tethers (Instech) to allow uninterrupted movement of the animals without disruption of infusion lines. Hyperinsulinemia was initiated by intravenous infusion of insulin (4 mU/kg/min). Blood was sampled from arterial lines at 7 min intervals and analyzed with a Beckman Glucose Analyzer II (Beckman Coulter). Euglycemia was maintained by variable infusion of 20% dextrose. Steady state was achieved approximately 90 min after initiating hyperinsulinemia and maintained for at least 45 min. Glucose infusion rates were calculated as the average glucose infusion rate during the steady-state period. Additional blood samples were taken before initiating hyperinsulinemia and at the end of the clamp for analysis of insulin and free fatty acids. [¹⁴C]glucose and [³H]2-DOG were given as a bolus during the steady-state period for estimation of hepatic glucose output and 2-DOG uptake, as previously described ([Ye et al., 2001](#)). Somatostatin (1.2 µg/kg/min) was coadministered with insulin in lipid-infused animals to prevent secretion of endogenous glucose in lard-oil-infused rats.

DES1 Knockout Mice

Mouse embryonic stem (ES) cells carrying a mutation in the *Des1* gene (accession number NM_007853) were obtained from OmniBank, a library of gene-trapped ES cell clones identified by a corresponding OmniBank sequence tag (OST) ([Zambrowicz et al., 1998](#)). The ES cell clone corresponding to OST 368559, matching the mouse *Des1* sequence, was thawed and expanded. Inverse genomic PCR analysis of DNA from this clone confirmed the insertion of the gene-trapping retroviral vector in the first intron of the *Des1* gene on chromosome 1, downstream of the translation initiation codon, thus

disrupting production of wild-type transcripts. OST 368559 cells were used to generate mice heterozygous for the *Des1* mutation. Genotyping was performed using oligonucleotide primers (LTR2, forward: 5'-AAATGGCGTTACTTAAGCTAGCTTGC-3'; gene-specific primer, reverse: 5'-AGCTAGTCACTCTGATTTCGAAAC-3') that were employed in a multiplex reaction to amplify mutant *Des1* alleles.

Lipid Infusion

Male Sprague-Dawley rats (~250 grams) were randomly divided into six different groups. Glycerol, 20% lard-oil, or 20% soy-oil emulsions were prepared as previously described ([Stein et al., 1997](#)) and infused at a constant rate of 5 ml/kg/hr. To activate lipoprotein lipase, heparin (6 U/hr) was added to the triglyceride emulsions. Lipids were infused in animals treated with control injections (normal saline) or myriocin (100 µg/kg, i.p.). Drugs were given 12 hr prior to lipid infusion, and equivalent doses were given intravenously at the time of infusion. Hyperinsulinemic-euglycemic clamps were initiated after 4.5 hr of lipid infusion by intravenous coinfusion of insulin for the duration of the procedure. Following lipid infusion, animals were deeply anesthetized with sodium pentobarbital, and soleus muscles and liver were rapidly dissected out and frozen in liquid nitrogen.

Isolated Muscles

Palmitate or linoleate was first dissolved in ethanol (200 mM), and ethanol or free fatty acids were conjugated to bovine serum albumin (BSA) by diluting 1:25 in Krebs-Henseleit buffer (KHB) supplemented with 20% BSA and heating (55°C for 30 min, with occasional vortexing). The final incubation medium was prepared by diluting the conjugated BSA solution 1:8 in freshly oxygenated KHB. Male Sprague-Dawley rats (150–200 grams) were deeply anesthetized with sodium pentobarbital (110 mg/kg, i.p.), and soleus muscles were isolated, laterally bisected, and transferred to 25 ml Erlenmeyer flasks containing 2 ml of KHB supplemented with 2.5% BSA, 8 mM glucose, and 1 mM HEPES (pH 7.2). Muscles were maintained in a shaking water bath at 29°C while being continuously gassed with 95% O₂/5% CO₂. Following this incubation, muscles were rapidly frozen in liquid nitrogen or stimulated with insulin (300 µU) for 60 min, and the incorporation of [³H]2-DOG was assessed during the final 20 min of the incubation using methods described previously ([Brozinick and Birnbaum, 1998](#)). Free fatty acids were present throughout the glucose uptake assay.

Zucker Diabetic Fatty Rats

Male ZDF rats were obtained from Charles River/Genetic Models, Inc. at 6 weeks of age. After a 2 week acclimation period, rats were pre-bled (~100 µl) and assigned to vehicle (1% w/v carboxymethylcellulose, 0.25% Tween 80) or myriocin (0.5 mg/kg/day) groups based on starting plasma glucose levels and body weight (day -1). Rats were administered compound daily by oral gavage between 8:30 and 9:30 am for 7 days. Blood samples were obtained 1 hr postdose at the indicated days from the tail vein of conscious animals by gentle massage following tail snip. Blood was collected in EDTA

tubes and kept chilled on ice. Following centrifugation of blood samples, plasma was used for measurements of glucose, insulin, and triglyceride levels. In a repeat analysis, ceramide was measured following treatment with myriocin (0.3 mg/kg every other day, i.p.) from 8 to 16 weeks of age.

Analysis of Metabolites

Insulin was measured by enzyme-linked immunosorbent assay (ELISA) using commercially available kits. For ZDF rats, plasma analytes were measured using a Hitachi 911 clinical chemistry analyzer (Roche). Free fatty acids were analyzed using a Free Fatty Acids Half-Micro Test Kit (Roche). Rat ceramide and diacylglycerol were enzymatically quantified as described previously ([Chavez et al., 2003](#)). Mouse ceramides were measured using mass spectrometry by the Lipidomics Core Facility at the Medical University of South Carolina. SPT2 protein was detected by immunoblotting with an antibody from Cayman Chemicals and quantified on a Kodak Image Station 2000R.

Quantitative Real-Time PCR

Total RNA was extracted and purified from tissues using TRIzol reagent (Invitrogen) according to the manufacturer's recommendations. Extracted RNA was solubilized in FORMAZOL and stored at -80°C until use. cDNA was synthesized from the mRNA by reverse-transcriptase PCR using a commercial cDNA synthesis kit with oligo(dT) primers (Promega). Quantitative real-time PCR was performed with SYBR Green Supermix (Bio-Rad) using a Bio-Rad iCycler system. Specific primer sequences are listed in [Table S1](#). PCR efficiency was examined by serially diluting the template cDNA, and a melt curve was performed at the end of each reaction to verify PCR product specificity. A sample containing no cDNA was used as a negative control to verify the absence of primer dimers. β -actin reactions were performed side by side with every sample analyzed. Changes in mRNA level of each gene for each treatment were normalized to that of the β -actin mRNA according to [Pfaffl \(2001\)](#). Ceramide synthase primers used to quantify mRNA levels were previously described ([Riebeling et al., 2003](#)).

Protein Analysis

Tissue extracts were resolved by SDS-PAGE, transferred to nitrocellulose, and immunoblotted using methods described previously ([Brozinick and Birnbaum, 1998](#)). Detection was performed using the Enhanced Chemiluminescence Plus kit from Amersham Biosciences according to the manufacturer's instructions. Rabbit polyclonal antibodies recognizing DES1 were custom produced by Rockland Immunochemicals by immunizing with the KLH-conjugated peptide C-RMKRPPKGNEILE, which encodes the enzyme's C terminus. IRS-1-associated PI3-kinase activity was analyzed as described previously ([Wang and Summers, 2003](#)). All other antibodies were from Cell Signaling.

Statistical Analysis

Data are presented as means \pm SEM. Statistical significance was determined by Student's t test when comparing two means or by one-way analysis of variance (ANOVA) when comparing multiple means. When statistical significance was detected by ANOVA, group differences were determined by Neuman-Keuls post hoc analyses. For glucose and insulin tolerance tests, statistical comparisons were made using the area under the curve. Analyses were performed using SAS/STAT software (SAS Institute Inc.).

Acknowledgments

The authors gratefully acknowledge the assistance of Michael Pagliassotti (Colorado State University) and Jared Rutter, Dale Abel, Deborah Jones, Robert Cooksey, and Don McClain (University of Utah). This work was supported by National Institutes of Health grants R01-DK58784 and R21-DK073181 to S.A.S. and F31-DK070565-03 to W.L.H., an American Diabetes Association Research Award to S.A.S., and American Heart Association postdoctoral and predoctoral fellowships to T.A.K. and K.L.H., respectively. G.K.F. is an employee and shareholder of Lexicon Genetics Inc. J.T.B., E.D.H., A.S., and S.K.K. are employees and shareholders of Eli Lilly and Co.

References

- [Adams et al., 2004](#) J.M. Adams 2nd, T. Pratipanawatr, R. Berria, E. Wang, R.A. DeFronzo, M.C. Sullards and L.J. Mandarino, Ceramide content is increased in skeletal muscle from obese insulin-resistant humans, *Diabetes* **53** (2004), pp. 25–31.
- [Boden and Shulman, 2002](#) G. Boden and G.I. Shulman, Free fatty acids in obesity and type 2 diabetes: defining their role in the development of insulin resistance and beta-cell dysfunction, *Eur. J. Clin. Invest.* **32** (2002) (Suppl 3), pp. 14–23. [Full Text via CrossRef](#)
- [Brozinick and Birnbaum, 1998](#) J.T. Brozinick Jr. and M.J. Birnbaum, Insulin, but not contraction, activates Akt/PKB in isolated rat skeletal muscle, *J. Biol. Chem.* **273** (1998), pp. 14679–14682.
- [Chavez and Summers, 2003](#) J.A. Chavez and S.A. Summers, Characterizing the effects of saturated fatty acids on insulin signaling and ceramide and diacylglycerol accumulation in 3T3-L1 adipocytes and C2C12 myotubes, *Arch. Biochem. Biophys.* **419** (2003), pp. 101–109. [Abstract](#) | [Full Text + Links](#) | [PDF \(275 K\)](#)
- [Chavez et al., 2003](#) J.A. Chavez, T.A. Knotts, L.P. Wang, G. Li, R.T. Dobrowsky, G.L. Florant and S.A. Summers, A role for ceramide, but not diacylglycerol, in the antagonism

of insulin signal transduction by saturated fatty acids, *J. Biol. Chem.* **13** (2003), pp. 10297–10303. [Full Text via CrossRef](#)

[Chavez et al., 2005](#) J.A. Chavez, W.L. Holland, J. Bar, K. Sandhoff and S.A. Summers, Acid ceramidase overexpression prevents the inhibitory effects of saturated fatty acids on insulin signaling, *J. Biol. Chem.* **280** (2005), pp. 20148–20153. [Full Text via CrossRef](#)

[Dobrzyn et al., 2004](#) A. Dobrzyn, M. Zendzian-Piotrowska and J. Gorski, Effect of endurance training on the sphingomyelin-signalling pathway activity in the skeletal muscles of the rat, *J. Physiol. Pharmacol.* **55** (2004), pp. 305–313.

[Gaster et al., 2005](#) M. Gaster, A.C. Rustan and H. Beck-Nielsen, Differential utilization of saturated palmitate and unsaturated oleate: evidence from cultured myotubes, *Diabetes* **54** (2005), pp. 648–656.

[Gorska et al., 2004](#) M. Gorska, A. Dobrzyn, M. Zendzian-Piotrowska and J. Gorski, Effect of streptozotocin-diabetes on the functioning of the sphingomyelin-signalling pathway in skeletal muscles of the rat, *Horm. Metab. Res.* **36** (2004), pp. 14–21.

[Hajduch et al., 2001](#) E. Hajduch, A. Balendran, I.H. Batty, G.J. Litherland, A.S. Blair, C.P. Downes and H.S. Hundal, Ceramide impairs the insulin-dependent membrane recruitment of protein kinase B leading to a loss in downstream signalling in L6 skeletal muscle cells, *Diabetologia* **44** (2001), pp. 173–183. [Full Text via CrossRef](#)

[Hannun and Obeid, 2002](#) Y.A. Hannun and L.M. Obeid, The ceramide-centric universe of lipid-mediated cell regulation: stress encounters of the lipid kind, *J. Biol. Chem.* **277** (2002), pp. 25847–25850. [Full Text via CrossRef](#)

[Helge et al., 2004](#) J.W. Helge, A. Dobrzyn, B. Saltin and J. Gorski, Exercise and training effects on ceramide metabolism in human skeletal muscle, *Exp. Physiol.* **89** (2004), pp. 119–127. [Full Text via CrossRef](#)

[Hermanowski-Vosatka et al., 2005](#) A. Hermanowski-Vosatka, J.M. Balkovec, K. Cheng, H.Y. Chen, M. Hernandez, G.C. Koo, C.B. Le Grand, Z. Li, J.M. Metzger and S.S. Mundt *et al.*, 11beta-HSD1 inhibition ameliorates metabolic syndrome and prevents progression of atherosclerosis in mice, *J. Exp. Med.* **202** (2005), pp. 517–527. [Full Text via CrossRef](#)

[Hojjati et al., 2005](#) M. Hojjati, Z. Li, H. Zhou, S. Tang, C. Huan, E. Ooi, S. Lu and X.C. Jiang, Effect of myriocin on plasma sphingolipid metabolism and atherosclerosis in apoE-deficient mice, *J. Biol. Chem.* **280** (2005), pp. 10284–10289 Published online December 6, 2004.

[Hotamisligil, 2003](#) G.S. Hotamisligil, Inflammatory pathways and insulin action, *Int. J. Obes. Relat. Metab. Disord.* **27** (2003) (Suppl 3), pp. S53–S55. [Full Text via CrossRef](#)

[Itani et al., 2002](#) S.I. Itani, N.B. Ruderman, F. Schmedier and G. Boden, Lipid-induced insulin resistance in human muscle is associated with changes in diacylglycerol, protein kinase C, and IkappaB-alpha, *Diabetes* **51** (2002), pp. 2005–2011.

[Kim et al., 2001](#) J.K. Kim, Y.J. Kim, J.J. Fillmore, Y. Chen, I. Moore, J. Lee, M. Yuan, Z.W. Li, M. Karin and P. Perret *et al.*, Prevention of fat-induced insulin resistance by salicylate, *J. Clin. Invest.* **108** (2001), pp. 437–446. [Full Text via CrossRef](#)

[Kim et al., 2004](#) J.K. Kim, J.J. Fillmore, M.J. Sunshine, B. Albrecht, T. Higashimori, D.W. Kim, Z.X. Liu, T.J. Soos, G.W. Cline and W.R. O'Brien *et al.*, PKC-theta knockout mice are protected from fat-induced insulin resistance, *J. Clin. Invest.* **114** (2004), pp. 823–827. [Full Text via CrossRef](#)

[Kim et al., 2002](#) Y.B. Kim, G.I. Shulman and B.B. Kahn, Fatty acid infusion selectively impairs insulin action on Akt1 and protein kinase C lambda /zeta but not on glycogen synthase kinase-3, *J. Biol. Chem.* **277** (2002), pp. 32915–32922. [Full Text via CrossRef](#)

[Kotelevtsev et al., 1997](#) Y. Kotelevtsev, M.C. Holmes, A. Burchell, P.M. Houston, D. Schmoll, P. Jamieson, R. Best, R. Brown, C.R. Edwards and J.R. Seckl *et al.*, 11beta-hydroxysteroid dehydrogenase type 1 knockout mice show attenuated glucocorticoid-inducible responses and resist hyperglycemia on obesity or stress, *Proc. Natl. Acad. Sci. USA* **94** (1997), pp. 14924–14929. [Full Text via CrossRef](#)

[Kotelevtsev et al., 1999](#) Y. Kotelevtsev, R.W. Brown, S. Fleming, C. Kenyon, C.R. Edwards, J.R. Seckl and J.J. Mullins, Hypertension in mice lacking 11beta-hydroxysteroid dehydrogenase type 2, *J. Clin. Invest.* **103** (1999), pp. 683–689.

[Masuzaki et al., 2001](#) H. Masuzaki, J. Paterson, H. Shinyama, N.M. Morton, J.J. Mullins, J.R. Seckl and J.S. Flier, A transgenic model of visceral obesity and the metabolic syndrome, *Science* **294** (2001), pp. 2166–2170. [Full Text via CrossRef](#)

[Masuzaki et al., 2003](#) H. Masuzaki, H. Yamamoto, C.J. Kenyon, J.K. Elmquist, N.M. Morton, J.M. Paterson, H. Shinyama, M.G. Sharp, S. Fleming and J.J. Mullins *et al.*, Transgenic amplification of glucocorticoid action in adipose tissue causes high blood pressure in mice, *J. Clin. Invest.* **112** (2003), pp. 83–90. [Full Text via CrossRef](#)

[McGarry, 2002](#) J.D. McGarry, Banting lecture 2001: dysregulation of fatty acid metabolism in the etiology of type 2 diabetes, *Diabetes* **51** (2002), pp. 7–18.

[Merrill, 2002](#) A.H. Merrill Jr., De novo sphingolipid biosynthesis: a necessary, but dangerous, pathway, *J. Biol. Chem.* **277** (2002), pp. 25843–25846. [Full Text via CrossRef](#)

[Olshansky et al., 2005](#) S.J. Olshansky, D.J. Passaro, R.C. Hershow, J. Layden, B.A. Carnes, J. Brody, L. Hayflick, R.N. Butler, D.B. Allison and D.S. Ludwig, A potential

decline in life expectancy in the United States in the 21st century, *N. Engl. J. Med.* **352** (2005), pp. 1138–1145. [Full Text via CrossRef](#)

[Pagliassotti et al., 2002](#) M.J. Pagliassotti, J. Kang, J.S. Thresher, C.K. Sung and M.E. Bizeau, Elevated basal PI 3-kinase activity and reduced insulin signaling in sucrose-induced hepatic insulin resistance, *Am. J. Physiol. Endocrinol. Metab.* **282** (2002), pp. E170–E176.

[Park et al., 2004](#) T.S. Park, R.L. Panek, S.B. Mueller, J.C. Hanselman, W.S. Rosebury, A.W. Robertson, E.K. Kindt, R. Homan, S.K. Karathanasis and M.D. Reikhter, Inhibition of sphingomyelin synthesis reduces atherogenesis in apolipoprotein E-knockout mice, *Circulation* **110** (2004), pp. 3465–3471. [Full Text via CrossRef](#)

[Pfaffl, 2001](#) M.W. Pfaffl, A new mathematical model for relative quantification in real-time RT-PCR, *Nucleic Acids Res.* **29** (2001), p. e45.

[Powell et al., 2003](#) D.J. Powell, E. Hajduch, G. Kular and H.S. Hundal, Ceramide disables 3-phosphoinositide binding to the pleckstrin homology domain of protein kinase B (PKB)/Akt by a PKCzeta-dependent mechanism, *Mol. Cell. Biol.* **23** (2003), pp. 7794–7808. [Full Text via CrossRef](#)

[Powell et al., 2004](#) D.J. Powell, S. Turban, A. Gray, E. Hajduch and H.S. Hundal, Intracellular ceramide synthesis and protein kinase C ζ activation play an essential role in palmitate-induced insulin resistance in rat L6 skeletal muscle cells, *Biochem. J.* **382** (2004), pp. 619–629.

[Reaven, 2005](#) G.M. Reaven, The insulin resistance syndrome: definition and dietary approaches to treatment, *Annu. Rev. Nutr.* **25** (2005), pp. 391–406.

[Riebeling et al., 2003](#) C. Riebeling, J.C. Allegood, E. Wang, A.H. Merrill Jr. and A.H. Futerman, Two mammalian longevity assurance gene (LAG1) family members, trh1 and trh4, regulate dihydroceramide synthesis using different fatty acyl-CoA donors, *J. Biol. Chem.* **278** (2003), pp. 43452–43459. [Full Text via CrossRef](#)

[Rivellese and Lilli, 2003](#) A.A. Rivellese and S. Lilli, Quality of dietary fatty acids, insulin sensitivity and type 2 diabetes, *Biomed. Pharmacother.* **57** (2003), pp. 84–87. [Abstract](#) | [Full Text + Links](#) | [PDF \(115 K\)](#)

[Schmitz-Peiffer, 2000](#) C. Schmitz-Peiffer, Signalling aspects of insulin resistance in skeletal muscle: mechanisms induced by lipid oversupply, *Cell. Signal.* **12** (2000), pp. 583–594. [Abstract](#) | [Full Text + Links](#) | [PDF \(677 K\)](#)

[Stein et al., 1997](#) D.T. Stein, B.E. Stevenson, M.W. Chester, M. Basit, M.B. Daniels, S.D. Turley and J.D. McGarry, The insulinotropic potency of fatty acids is influenced profoundly by their chain length and degree of saturation, *J. Clin. Invest.* **100** (1997), pp. 398–403.

[Straczkowski et al., 2004](#) M. Straczkowski, I. Kowalska, A. Nikolajuk, S. Dzienis-Straczkowska, I. Kinalska, M. Baranowski, M. Zendzian-Piotrowska, Z. Brzezinska and J. Gorski, Relationship between insulin sensitivity and sphingomyelin signaling pathway in human skeletal muscle, *Diabetes* **53** (2004), pp. 1215–1221.

[Stratford et al., 2001](#) S. Stratford, D.B. DeWald and S.A. Summers, Ceramide dissociates 3'-phosphoinositide production from pleckstrin homology domain translocation, *Biochem. J.* **354** (2001), pp. 359–368. [Full Text via CrossRef](#)

[Stratford et al., 2004](#) S. Stratford, K.L. Hoehn, F. Liu and S.A. Summers, Regulation of insulin action by ceramide: dual mechanisms linking ceramide accumulation to the inhibition of Akt/protein kinase B, *J. Biol. Chem.* **279** (2004), pp. 36608–36615. [Full Text via CrossRef](#)

[Summers and Nelson, 2005](#) S.A. Summers and D.H. Nelson, A role for sphingolipids in producing the common features of type 2 diabetes, metabolic syndrome X, and Cushing's syndrome, *Diabetes* **54** (2005), pp. 591–602.

[Summers et al., 1998](#) S.A. Summers, L.A. Garza, H. Zhou and M.J. Birnbaum, Regulation of insulin-stimulated glucose transporter GLUT4 translocation and Akt kinase activity by ceramide, *Mol. Cell. Biol.* **18** (1998), pp. 5457–5464.

[Teruel et al., 2001](#) T. Teruel, R. Hernandez and M. Lorenzo, Ceramide mediates insulin resistance by tumor necrosis factor-alpha in brown adipocytes by maintaining Akt in an inactive dephosphorylated state, *Diabetes* **50** (2001), pp. 2563–2571.

[Turinsky et al., 1990](#) J. Turinsky, D.M. O'Sullivan and B.P. Bayly, 1,2-Diacylglycerol and ceramide levels in insulin-resistant tissues of the rat in vivo, *J. Biol. Chem.* **265** (1990), pp. 16880–16885.

[Wakelam, 1998](#) M.J. Wakelam, Diacylglycerol—when is it an intracellular messenger?, *Biochim. Biophys. Acta* **1436** (1998), pp. 117–126. [Abstract](#) | [Full Text + Links](#) | [PDF \(211 K\)](#)

[Wang et al., 1998](#) C.-N. Wang, L. O'Brien and D.N. Brindley, Effects of cell-permeable ceramides and tumor necrosis factor- α on insulin signaling and glucose uptake in 3T3-L1 adipocytes, *Diabetes* **47** (1998), pp. 24–31.

[Wang and Summers, 2003](#) L.P. Wang and S.A. Summers, Measuring insulin-stimulated phosphatidylinositol 3-kinase activity, *Methods Mol. Med.* **83** (2003), pp. 127–136. [Full Text via CrossRef](#)

[Ye et al., 2001](#) J.M. Ye, P.J. Doyle, M.A. Iglesias, D.G. Watson, G.J. Cooney and E.W. Kraegen, Peroxisome proliferator-activated receptor (PPAR)-alpha activation lowers muscle lipids and improves insulin sensitivity in high fat-fed rats: comparison with

PPAR-gamma activation, *Diabetes* **50** (2001), pp. 411–417. [Abstract](#) | [Full Text + Links](#) | [PDF \(323 K\)](#)

[Yu et al., 2002](#) C. Yu, Y. Chen, G.W. Cline, D. Zhang, H. Zong, Y. Wang, R. Bergeron, J.K. Kim, S.W. Cushman and G.J. Cooney *et al.*, Mechanism by which fatty acids inhibit insulin activation of insulin receptor substrate-1 (IRS-1)-associated phosphatidylinositol 3-kinase activity in muscle, *J. Biol. Chem.* **277** (2002), pp. 50230–50236. [Full Text via CrossRef](#)

[Zambrowicz et al., 1998](#) B.P. Zambrowicz, G.A. Friedrich, E.C. Buxton, S.L. Lilleberg, C. Person and A.T. Sands, Disruption and sequence identification of 2,000 genes in mouse embryonic stem cells, *Nature* **392** (1998), pp. 608–611. [Full Text via CrossRef](#)

Supplemental Data



(259 K)

[mmc1.pdf](#)  [Help](#)

Acrobat PDF file 1.

Document S1. One Table and Seven Figures.



Corresponding author